Published in final edited form as:
Cancer Cell. 2011 November 15; 20(5): 661–673. doi:10.1016/j.ccr.2011.10.012.

IL-6 controls leukemic multipotent progenitor cell fate and contributes to chronic myelogenous leukemia development

Damien Reynaud[1,*], **Eric Pietras**[1], **Keegan Barry-Holson**[1], **Alain Mir**[2], **Mikhail Binnewies**[1], **Marion Jeanne**[1], **Olga Sala-Torra**[3], **Jerald P. Radich**[3], and **Emmanuelle Passegué**[1,*]

[1]The Eli and Edythe Broad Center of Regenerative Medicine and Stem Cell Research, Department of Medicine, Division of Hematology/Oncology, University of California San Francisco, San Francisco, California, 94143, USA.

[2]Fluidigm Corporation, South San Francisco, California, 94080, USA

[3]Clinical Research Division, Fred Hutchinson Cancer Research Center, Seattle, Washington 98109, USA

Abstract

Using a mouse model recapitulating the main features of human chronic myelogenous leukemia (CML), we uncover the hierarchy of leukemic stem and progenitor cells contributing to disease pathogenesis. We refine the characterization of CML leukemic stem cells (LSCs) to the most immature long-term hematopoietic stem cells (LT-HSCs) and identify some important molecular deregulations underlying their aberrant behavior. We find that CML multipotent progenitors (MPPs) exhibit an aberrant B-lymphoid potential but are redirected towards the myeloid lineage by the action of the pro-inflammatory cytokine IL-6. We show that BCR/ABL activity controls *Il-6* expression thereby establishing a paracrine feedback loop that sustains CML development. These results describe how pro-inflammatory tumor environment affects leukemic progenitor cell fate and contributes to CML pathogenesis.

INTRODUCTION

Chronic myelogenous leukemia (CML) is a clonal myeloproliferative neoplasm (MPN) characterized by the t(9;22)(q34;q11) reciprocal translocation, which leads to the expression of the *BCR/ABL* fusion protein (Savona and Talpaz, 2008). BCR/ABL is a hyperactive and deregulated tyrosine kinase that promotes leukemic growth by disrupting of a broad range of signaling pathways involved in cell survival, proliferation, and differentiation. Clinically, the natural course of the disease includes three distinct phases (Perrotti et al., 2010). The initial phase is characterized by a progressive myeloid expansion, with accumulation of myeloid progenitors and mature granulocytes in the bone marrow (BM) and peripheral blood (PB). Upon acquisition of secondary mutations, this chronic phase evolves through an accelerated phase into an acute leukemia-like blast crisis involving either myeloid, B lymphoid or myeloid/lymphoid biphenotypic cells. During the chronic phase, CML cells

[*]Co-corresponding authors: Emmanuelle Passegué, PhD (passeguee@stemcell.ucsf.edu) Damien Reynaud, PhD (reynaudd@stemcell.ucsf.edu) University of California San Francisco 35 Medical Way, Regeneration Medicine Building (RMB), Rm. 1017, Box 0667 San Francisco, CA 94143, USA Phone: 415-476-2426 Fax: 415-476-9273.

have been shown to be functionally heterogeneous and capable of maintaining a hierarchical organization caricaturing normal hematopoiesis, with only a fraction of the cells being actually responsible for disease maintenance and propagation, thus behaving as leukemia-initiating stem cells (LSCs) (Passegué and Weissman, 2005).

The existence of a LSC compartment has fundamental consequences for CML therapy (Savona and Talpaz, 2008). While BCR/ABL tyrosine kinase inhibitors (TKIs) are remarkably effective in inducing remission in chronic phase patients, they are not effective against CML-LSCs, which can persist and regenerate the disease upon drug discontinuation. Why CML-LSCs are refractory to TKIs remains a matter of debate. One explanation could be a failure to achieve an efficient therapeutic concentration of TKIs in CML-LSCs due to their particular location in protective niches, their high content of drug efflux pumps and/or their enhanced expression of *BCR/ABL* (Barnes and Melo, 2006). A recent study suggests an alternative scenario wherein CML-LSCs are not killed by TKIs as other CML cells because they are actually insensitive to BCR/ABL inhibition (Corbin et al., 2011). This model predicts that BCR/ABL-based therapies will not eliminate CML-LSCs and highlights the need for approaches targeting alternative pathways that are critical for LSCs maintenance. A refined characterization and better understanding of CML-LSC biology is therefore essential for the establishment of targeted anti-LSC therapies and the development of curative treatment for CML.

Historically, BCR/ABL retroviral transduction/transplantation studies in the mouse have been instrumental in showing that BCR/ABL is the direct cause of CML and in validating this oncogene as a drug target. Furthermore, these studies were used to demonstrate that CML-LSCs are contained in the hematopoietic stem cell (HSC) enriched $Lin^{-}/Sca\text{-}1^{+}/c\text{-}Kit^{+}$ (LSK) fraction of the BM (Hu et al., 2006), and that developmental pathways controlling HSC function are essential for CML-LSCs generation and CML development (Warr et al., 2011). However, such experimental approaches have inherent limitations due to the constraints imposed by the retroviral transduction, and the use of irradiated recipients for transplantation. In this context, the *Scl/Tal1-tTA x TRE-BCR/ABL* double transgenic mice, which allow for inducible *BCR/ABL* expression in HSCs and CML development in adult mice (Koschmieder et al., 2005), represent a valuable alternative to study CML pathogenesis and to test therapies *in vivo* (Zhang et al., 2010). Here, we used this inducible *BCR/ABL* transgenic mouse model to understand the effect of BCR/ABL activity on hematopoietic development.

RESULTS

CML development is associated with a profound re-organization of BM hematopoiesis

Scl/Tal1-tTA and *TRE-BCR/ABL* transgenic mice were bred in the presence of doxycycline, and *BCR/ABL* (*BA*$^{+}$) expression was induced by doxycycline withdrawal 5 weeks after birth (Figure 1A). All induced double transgenic mice (thereafter called *BA* mice) progressively developed a CML-like disease associated with a severe myeloid cell expansion and reduction in B and T cell lineages in the BM, spleen and PB (Figures 1A, 1B and S1A), and splenomegaly (Figure 1C). *BA* mice also became moribund ~ 6 weeks after induction. In contrast to other genetic backgrounds (Koschmieder et al., 2005), no lymphoid disorders were observed in over 100 *BA* mice on a pure C57Bl/6 background. CML development in 5-6 weeks induced *BA* mice was associated with a 2-fold reduction in BM cellularity (Figure 1D) and the development of a profound myelofibrosis (Figure 1E, F), as previously described in ~ 30% of CML patients (Buesche et al., 2007). Analysis of the LSK compartment showed a severe reduction in the number of LT-HSCs ($LSK/Flk2^{-}/CD48^{-}/CD150^{+}$) and ST-HSCs ($LSK/Flk2^{-}/CD48^{-}/CD150^{-}$), which was accompanied by an expansion of the non-self-renewing $CD48^{+}$ cells ($LSK/Flk2^{-}/CD48^{+}$), while the number of

MPPs (LSK/Flk2$^+$) remained unchanged (Figures 1D and S1B). Analysis of the myeloid progenitor compartment indicated a severe reduction in the number of common myeloid progenitors (CMP: LK/CD34$^+$/FcγR$^-$) and megakaryocyte/erythrocyte progenitors (MEP: LK/CD34$^-$/FcγR$^-$), while the number of granulocyte/macrophage progenitors (GMP: LK/CD34$^+$/FcγR$^+$) remained unchanged and fueled CML development (Figures 1D and S1B). Finally, the reduction in lymphoid-lineage cells was correlated with a ~ 8-fold decrease in the numbers of common lymphoid progenitors (CLP: Lin$^-$/c-Kit^{low}/Sca1^{low}/Flk2$^+$/IL7Rα$^+$) (Figures 1D). These BM changes were also associated with the development of an extramedullary hematopoiesis in the spleen affecting all immature compartments, except for CLPs (Figures 1C and 1D). Altogether, these results indicate a profound hematopoietic remodeling in response to CML development characterized by the loss of the immature stem and progenitor compartments in the BM, and their compensatory increase and redistribution to peripheral organs.

BCR/ABL alters the biology of several stem and multipotent progenitor cells

To assess how BCR/ABL activity affects the biological output of specific BM populations, we transplanted highly purified stem and progenitor cells isolated from 5-6 weeks induced *BA* mice into sub-lethally irradiated congenic recipients (Figure 2A). As expected, transplantation of *BA*$^+$ myeloid-committed CMPs and GMPs (Huntly et al., 2004), but also of lymphoid-committed CLPs, failed to sustain lasting chimerism in the PB, BM and spleen and to transplant the disease (Figures 2B, 2C and S2A). Similarly, transplantation of the two most abundant populations present in the LSK compartment (*i.e.*, MPPs and the expanded CD48$^+$ cells) failed to transfer CML, although transplantation of *BA*$^+$ MPPs led to a high degree of chimerism due to a massive production of B cells (Figure S2B). In contrast, transplantation of either *BA*$^+$ LT-HSCs or ST-HSCs (4,000 cells/mouse) both induced the development of a robust CML disease, with the transplanted mice becoming moribund within one month post-transplantation (Figures 2B). Analyses of these mice showed a clear bias toward myeloid cell production in the BM, spleen and PB (Figures 2C and S2A and S2B), together with a severe reorganization of the stem and progenitor compartments in the BM (*i.e.*, increased percentage of CD48$^+$ cells and GMPs) (Figure 2D), infiltration of mature myeloid cells in the liver (Figure S2C), and development of splenic extramedullary hematopoiesis (data not shown). Taken together, these results show that transplantation of either LT-HSCs or ST-HSCs recapitulates the core features of the CML disease observed in primary *BA* mice, and suggest that two distinct stem cell populations present in the LSK compartment may function as LSCs, at least at high doses of transplanted cells.

Refining the identity of CML-LSCs

LT- and ST-HSCs are functionally defined by the extent of their self-renewal capacity (Benveniste et al., 2010). To investigate how such functional distinctions translated in the context of CML leukemogenesis, we performed transplantation in limiting conditions into sub-lethally irradiated recipients (Figure 3A). Although transplantation of either 500 control or *BA*$^+$ LT-HSCs or ST-HSCs gave rise to similar levels of PB chimerism, only *BA*$^+$ LT-HSCs maintained an elevated production of myeloid cells that ultimately led to CML development and death of the recipient mice (93 ± 6 days; n=3). In contrast, *BA*$^+$ ST-HSCs only promoted a transient myeloid hyperplasia that resulted in the same percentage of circulating myeloid cells than control ST-HSCs by 50 days post-transplantation. We also transplanted 50 control or *BA*$^+$ LT-HSCs into sub-lethally irradiated recipients to better quantify the number of CML-LSCs present in the LT-HSC compartment (Figure 3B). While we did not observe significant engraftment from control LT-HSCs under these highly competitive conditions, 6 of the 7 mice transplanted with 50 *BA*$^+$ LT-HSCs showed a robust (37.9 ± 4.5 %) and long-lasting (>20 weeks) multilineage PB chimerism. Moreover, 5 of the 6 engrafted mice developed CML and become moribund with a latency of 159 ± 24 days,

indicating that 1 out of 40 BA^+ LT-HSCs (calculated according to Poisson statistics, data not shown) is a *bona fide* CML-LSC. Strikingly, BM analysis of diseased mice showed that CML-LSCs were able to completely out-compete the normal hematopoiesis re-emerging from irradiated recipients (Figure 3C). Altogether, these results demonstrate that CML-LSCs reside exclusively within the LT-HSC compartment and display a massive competitive advantage at the clonal level. They also indicate that BA^+ ST-HSCs function as a short-term leukemic progenitor compartment, which amplifies the myeloid hyperplasia in a manner that might eventually be fatal upon transplantation of large numbers of cells, but which cannot *per se* sustain long-term CML development.

Aberrant features and molecular deregulations in CML-LSCs

We next investigated how BCR/ABL impacts on the molecular networks controlling LT-HSC function. We observed a striking hyperproliferative phenotype in BA^+ LT-HSCs (Figure 3D), which was characterized by a significant loss of quiescence and a 2-fold increase in proliferation rates. We then used a Fluidigm Dynamic RT-PCR array to perform a detailed quantitative expression analysis of 96 genes of interest in pools (n=7) of 100 control and BA^+ LT-HSCs (Figure 3F). Consistent with their increased proliferation, expression of the G_2/M cyclins A2 (*Ccna2*) and B1 (*Ccnb1*), and their associated cyclin-dependent kinase 1 (*Cdk1*), was elevated in BA^+ LT-HSCs. We also observed decreased expression of the early G_1 cyclin D1 (*Ccnd1*) and cyclin-dependent kinase inhibitor p57 (*Cdkn1c*) in BA^+ LT-HSCs, similar to what we have already reported in another population of LT-HSC-derived LSCs in *jun*B-deficient CML-like mice (Santaguida et al., 2009). Focusing on self-renewal programs, we confirmed the previously described down-regulation of *Evi1* and *Mpl* expression in BA^+ LT-HSCs (Schemionek et al., 2010), and found no significant changes in the expression levels of *Bmi1*, *Pten*, *Hoxb4*, *Ikzf1* (*Ikaros*) and *GATA2* (Figure 3G). Strikingly, we uncovered major alterations in the regulation of the Notch pathway, with significant reduction in the expression of both *Notch1* and its transcriptional target *Hes1* in BA^+ LT-HSCs. Taken together, these results indicate that CML-LSCs have a hyperproliferative phenotype that occurs without loss of self-renewal activity, and leads to clonal dominance. They also suggest that impairment of the Notch signaling pathway could contribute to the aberrant proliferation and myeloid cell production from CML-LSCs as previously reported for *jun*B-deficient LSCs (Santaguida et al., 2009) and more recently described in other MPN models (Klinakis et al., 2011).

Transient B cell hyperplasia arising from leukemic MPPs

While both BA^+ LT-HSCs and ST-HSCs have an extensive ability to produce myeloid cells, transplantation of BA^+ MPPs promotes a surprising B cell overproduction (Figures 2B, 2C and S2B). To analyze this phenomenon, we transplanted control or BA^+ MPPs (4,000 cells/mouse) into sub-lethally irradiated recipients (Figure 4A). Analyses performed at 35 days post-transplantation showed dramatically elevated BM chimerism in mice transplanted with BA^+ MPPs compared to control MPPs, which consisted mainly of $B220^+$ donor-derived B cells and reflected a specific increase in $CD43^+$ pro-B cells with corresponding decreased in $CD43^-$ pre-B and IgM^+ immature/mature B cells (Figure 4B). This dramatic increase in pro-B cell production from BA^+ MPPs was able to completely repress hematopoietic recovery from sub-lethally irradiated recipient mice (Figure S3A). Consistent with this major hematopoietic disruption, 2 out of 7 transplanted mice were anemic and moribund when analyzed, while the other mice developed extensive splenic extramedullary hematopoiesis and survived (data not shown). This pro-B cell hyperplasia was specific to the leukemic MPP compartment, as the output of the downstream CLP compartment was not similarly affected by BCR/ABL activity (Figure 2C and data not shown). In addition, it did not correspond to the development of B cell acute lymphoblastic leukemia (B-ALL), as the pro-B cell hyperplasia remained restricted to the BM (Figures S3B and S3C), was not

transplantable to secondary recipients (data not shown). Most notably, this hyperplasia did not persist over time and was absent in the surviving mice by 70 days post-transplantation (Figure 4B). Altogether, these results indicate that BCR/ABL increases and biases the differentiation potential of MPPs towards the production of B cell progenitors at the expense of myeloid cell generation, but without promoting its oncogenic transformation.

Context-dependent behavior of leukemic MPPs

Although we observed an extensive B-lymphoid potential in transplanted *BA*$^+$ MPPs, primary *BA* mice displayed a reduced B cell compartment (Figure 1B). To address this paradox, we co-transplanted 4,000 *BA*$^+$ MPPs together with 4,000 *BA*$^+$ HSCs (either long-term or short-term) into sub-lethally irradiated recipients (Figure 4C). Strikingly, 35 days after co-transplantation, 4 out of 5 recipient mice developed a CML disease (Figure 4C), which indicated that pathological myeloid expansion driven by *BA*$^+$ HSCs was able to repress the B cell expansion promoted by leukemic MPPs. We then analyzed the biological properties and molecular regulation of MPPs isolated from primary CML-developing *BA* mice. Consistent with their extensive reconstitution activity upon transplantation, *BA*$^+$ MPPs exhibit a 2-fold increase in proliferation rates (Figure 4D). Gene expression analyses of *BA*$^+$ MPPs only revealed marginal changes for genes encoding cell cycle regulators (Figures S3D). In contrast we observed a striking increase in the expression levels of myeloid determinants such as *Irf8* or *Csf1r* (*M-CSFR*), and a concomitant decrease in the expression of key lymphoid determinants including *Notch1*, *Hes1*, *Gfi1*, *Ikzf1* (*Ikaros*) and *Tcf3* (*E2A*) in *BA*$^+$ MPPs (Figure 4E). Taken together, these results indicate that *BA*$^+$ MPPs are intrinsically poised toward B lymphoid differentiation but are reprogrammed toward the myeloid fate during CML development, hence revealing an un-expected context-dependent behavior for these leukemic MPPs.

CML-driven IL-6 production suppresses lymphoid differentiation from leukemic MPPs

We reasoned that molecular effectors responsible for the fate reprogramming of leukemic MPPs could be extracellular signaling molecules detectable in the serum of CML-developing mice. Analyses performed with an antibody-based protein array revealed increased levels of a number of cytokines and growth factors in the serum of primary *BA* mice (Figure 5A). We focused on the multifunctional pro-inflammatory cytokine interleukin-6 (IL-6), which has been previously implicated in both myeloid expansion and lymphocytopenia (Maeda et al., 2005). Using an enzyme-linked immunoabsorbent assay (ELISA) on sera and spleen homogenates, we confirmed increased IL-6 concentrations in all CML-developing mice, either primary *BA* mice or *BA*$^+$ HSCs transplanted mice (Figure 5B). qRT-PCR analyses demonstrated that the expanded myeloid CML cells were the major source of IL-6 production during disease development (Figure 5C), while flow cytometry studies indicated that the receptor for IL-6 (IL-6Rα) was detectable on both control and *BA*$^+$ MPPs and downstream myeloid progenitors, but not on the most immature LT-HSCs or ST-HSCs (Figure 5D). Strikingly, addition of murine recombinant IL-6 completely blocked the ability of *BA*$^+$ MPPs to generate CD19$^+$ B cells in *in vitro* culture (Figure 5E). In addition, IL-6 dramatically increased the numbers and size of myeloid colonies generated from *BA*$^+$ MPPs in methylcellulose clonogenic assays, while no significant effects were observed from *BA*$^+$ GMP in the same conditions (Figure 5F). Taken together, these results indicate that the IL-6 secreted by the expanded myeloid CML cells directly acts on leukemic MPPs and re-directs their aberrant *BCR/ABL*-driven intrinsic B cell potential towards the myeloid lineage (Figure 5G).

In vivo cross-talk between leukemic and non-leukemic hematopoietic compartments

In CML patients, the leukemic cells co-exist and compete with normal hematopoiesis. To model such interactions and validate the function of IL-6 in these relevant conditions, we co-

transplanted 2×10^6 wild type (WT: CD45.2 GFP^+) along with 2×10^6 non-induced *BA* (CD45.2 GFP^-) unfractionated BM cells into lethally irradiated recipients (CD45.1 GFP^-) maintained under doxycycline (Figure 6A). As expected, WT and non-induced *BA* cells showed a similar 50:50 chimerism at 2 months post-transplantation (Figure 6B). Upon doxycycline withdrawal, 4 of 5 transplanted mice developed CML with disease onset ranging from 40 to 154 days (median 99 days; n=4). Strikingly, the 50:50 chimerism was preserved in CML-developing mice, with both WT and BA^+ cells contributing to the expanded mature myeloid cells (Figure 6B). We confirmed increased concentrations of IL-6 in the serum of CML-developing mice (Figure 6C). Interestingly while BA^+ cells were over-represented within the LT-HSC and ST-HSC compartments (85.8% ± 5.1 and 82.4% ± 6.1 respectively; mean ± SEM; n=2), the MPP compartment displayed an equal contribution of BA^+- and WT-derived cells (50.9% ± 1.3 BA^+ cells, mean ± SEM, n=2) similar to the 50:50 chimerism found in the expanded myeloid lineage. Taken together, these results confirm *in vivo* that lineage determination can be controlled by systemic factors downstream of CML-LSCs, and correlate the increase in IL-6 production driven by myeloid CML cells with the re-routing of both leukemic and normal MPPs towards the myeloid lineage.

IL-6 contributes to CML development

To confirm the function of IL-6 in CML pathogenesis, we evaluated disease progression in the absence of IL-6 signaling by crossing our *BA* mice with *Il-6*$^{-/-}$ mice (Kopf et al., 1994). Upon doxycycline withdrawal, both *BA Il-6*$^{-/-}$ and *BA Il-6*$^{+/-}$ mice displayed significantly increased overall survival compared to *BA Il-6*$^{+/+}$ mice (Figure 7A). Consistent with IL-6 serum concentrations (Figure 7B), we observed a stepwise decreased in myeloid cell production together with a stepwise recovery of B cell generation in the BM of *BA Il-6*$^{+/-}$ and *Il-6*$^{-/-}$ mice (Figure 7C). These effects were specific to *Il-6* inactivation since disruption of other cytokine signaling pathways, such as GM-CSF signaling, in *BA* mice did not affect CML development (data not shown). Interestingly, the lymphoid restoration observed in *BA Il-6*$^{-/-}$ mice also displayed aberrant pro-B cell features (Figure 7C) similar to the pro-B cell expansion observed upon transplantation of purified BA^+ MPPs (Figure 3B). In addition, *BA Il-6*$^{-/-}$ mice maintained a high level of myeloid cells circulating in the PB due to their extensive extramedullary hematopoiesis (data not shown), and eventually succumb to late onset CML diseases without developing overt lymphoid malignancies. Altogether, these results demonstrated that IL-6 signaling normally blocks the aberrant *BCR/ABL*-driven pro-B cell potential of leukemic MPPs and enhances myeloid differentiation, hence leading to a positive feedback loop promoting CML development. They also indicate that IL-6 blocking strategy can significantly delay CML onset in situations where BCR/ABL remains active.

BCR/ABL controls *Il-6* expression in myeloid CML cells

Finally, we investigated the mechanisms controlling IL-6 production using human leukemic cell lines and samples from CML patients. *BCR/ABL*-expressing K562 erythroleukemic cells and HL60 promyelocytic leukemia cells engineered to stably express *BCR/ABL* (Porosnicu et al., 2001) displayed high levels of *IL-6* mRNA, which could be rapidly downregulated by inhibition of BCR/ABL activity with TKIs (Imatinib or Dasatinib) (Figure 8A). This effect was specific to *IL-6* since the expression of *BCR/ABL* and other components of the IL-6 signaling pathway, including *IL-6Ra,* were not similarly affected by TKI treatment. For both cell lines, ELISA analyses confirmed that changes in *IL-6* gene expression correlated with changes in the levels of IL-6 protein secreted in the culture supernatant (Figure 8B). We then investigated TKI-treated K562 cells for expression of a panel of effectors genes known to regulate *IL-6* expression (Figure 8C). We found a significant downregulation of both *LIN28* and*LIN28b* expression and a considerable increase in *BCL6* expression. BCL6 is a direct transcriptional repressor of the *IL-6* gene (Yu et al., 2005), and recent work has shown that BCR/ABL-driven STAT5 activation inhibits *BCL6* expression (Duy et al., 2011).

Although the regulation of *LIN28/28b* by BCR/ABL is still largely unknown, they have been shown to inhibit the maturation of the *Let-7* microRNA, which is itself a negative regulator of *IL-6* expression (Iliopoulos et al., 2009). Therefore, we propose that pharmacological inhibition of BCR/ABL activity increased BCL6 levels and, as shown here, decreased LIN28/28b levels (Figure 8C), which could both contribute to the downregulation of *IL-6* expression observed in TKI-treated K562 cells (Figure 8D). *BCR/ABL* levels have also been shown to increase with disease progression (Savona and Talpaz, 2008) and elevated levels of IL-6 protein have been observed in the serum of accelerated and myeloid blasts crisis patients (Anand et al., 1998). Consistently, we observed a striking upregulation of *IL-6* expression during CML development in a large cohort of chronic, accelerated and blast crisis phase CML samples analyzed by microarray (Figure 8E). Furthermore, we noticed an accompanying decreased in BCL6 expression, particularly in blast crisis samples (Figure 8E), while upregulation of LIN28 during CML progression has been previously reported (Viswanathan et al., 2009). Taken together, these results demonstrate that BCR/ABL activity controls *IL-6* expression in myeloid CML cells, and suggest that both BCL6 and LIN28/28b are involved in the complex molecular network mediating this effect.

DISCUSSION

In this study, we use an inducible *BCR/ABL* transgenic mouse model that recapitulates the main features of human chronic phase CML. This allows us to considerably improve on the phenotypic and functional characterization of CML-LSCs, and to segregate them from two newly identified non-self-renewing leukemic multipotent progenitor populations that are present in the LSK fraction of the BM. These results unambiguously prove the longstanding concept that CML arise from transformed HSCs, and demonstrate that the clinically relevant CML-LSCs are solely contained in the rare LT-HSC compartment. This finding is essential to identify therapeutic targets that are specific to CML-LSCs and not to the most abundant leukemic multipotent progenitors, as currently done with the loose LSK definition of CML-LSCs. Moreover, we describe how leukemic multipotent progenitors contribute to CML development, and the essential function played by the pro-tumorigenic inflammatory environment in controlling disease pathogenesis.

CML-LSCs

Here, we demonstrate that CML-LSCs are exclusively contained in the rare LT-HSC compartment, which represent less that 10% of the LSK BM fraction (Warr et al., 2011). This level of resolution allows us to investigate the aberrant features that are specific to CML-LSCs, and to identify key deregulated mechanisms that could be amendable to targeted therapy. Based on phenotypic analysis and serial transplantation of *BCR/ABL*-expressing LSK cells, it has been recently suggested that BCR/ABL activity induces loss of HSC self-renewal capacity and promotes differentiation (Schemionek et al., 2010). Indeed, we observe a profound reorganization of the LSK BM compartment following CML development, with a severe reduction in the numbers LT-HSCs, ST-HSCs and expansion of non-self-renewing LSK/Flk2^{-}/CD48^{+} cells and Flk2^{+} MPPs. However, we find that such changes in the BM are associated with the development of a massive myelofibrosis, and are fully compensated for by the emergence of extramedullary hematopoiesis with increased numbers of LT-HSCs in the spleen. Most importantly, we observe that *BCR/ABL*-expressing LT-HSCs are able to self-renew extensively and to out-compete normal LT-HSCs, both in stress conditions upon transplantation in sub-lethally irradiated recipients, and in steady-state conditions when *BCR/ABL* expression is induced in transplanted mice harboring chimeric hematopoiesis. This property is consistent with the clonal dominance observed in human CML patients, where the majority of CD34^{+} stem and progenitor cells carry the BCR/ABL translocation (Holyoake et al., 1999). These findings are also in line with our

recent findings in the *jun*B-deficient CML-like model, where increase proliferation in transformed LT-HSCs is also not associated with a loss of self-renewal capacity (Santaguida et al., 2009). Consistent with this idea, BCR/ABL activity does not dramatically disrupt the transcriptional networks regulating LT-HSC self-renewal. More strikingly, we observe significant changes in cell cycle machinery and decrease expression of Notch signaling components in *BCR/ABL*-expressing LT-HSCs that are similar to the deregulations we previously described in *jun*B-deficient LT-HSCs (Santaguida et al., 2009). These findings reinforce the idea that deregulation of the Notch pathway is a key contributor to aberrant myelopoiesis (Klinakis et al., 2011), and that loss of quiescence and resulting hyperproliferation in transformed LT-HSCs may occur through a dampening of the cyclin D1/Cdkn1c (p57) regulatory axis (Pietras et al., 2011). They also suggest that LT-HSC transformation may, in fact, result from the perturbation of a few common regulatory pathways regardless of the initiating oncogenic event and that strategy aimed at restoring Notch activity in transformed LT-HSCs may represent a valid therapeutic approach to targeted LSC aberrant activity in CML and other type of MPNs.

CML multipotent progenitors

Here, we also demonstrate that *BCR/ABL* expression affects the activity of ST-HSCs and MPPs, but not of any other tested lineage-committed progenitors. BCR/ABL activity increases cell cycling and considerably expands the output of both ST-HSCs and MPPs, thereby providing these leukemic progenitors with extensive, although transient, *in vivo* reconstitution ability upon transplantation. Strikingly, opposite lineage outputs were generated from these transplanted cells, with leukemic ST-HSCs, like CML-LSCs, giving rise to a generalized myeloid hyperplasia, and leukemic MPPs producing a massive accumulation of pro-B cells in the BM. These results indicate that BCR/ABL exerts cell-type specific effects and biases the lineage potential of specific multipotent progenitor cells based on their stage of maturation and, likely, the permissiveness of their molecular programming. These results highlight the fact that CML develops from transformed LT-HSCs through a continuum of leukemic progenitor cells that are devoid of self-renewal activity but have defined aberrant properties. As we observe here, such non self-renewing leukemic progenitors can easily kill a mouse when transplanted at high doses and generate a disease, which despite being not transplantable, closely mimics CML both in kinetic and phenotype. This can have a confusing effect especially when transplanting high numbers of transduce mix populations such as 5-FU treated BM or LSK cells. Caution should therefore be taken in interpreting the results of retroviral transduction/transplantation experiments, particularly when assessing the effect on CML-LSC numbers through serial transplantations, and on the myeloid/lymphoid nature of the emerging CML disease.

Pro-tumorigenic inflammatory environment in CML pathogenesis

Our results unveil an essential paracrine mechanism involving the pro-inflammatory cytokine IL-6, which serves as a positive feedback loop to sustain CML development and acts at the level of leukemic MPPs by reprogramming them towards myeloid development at the expense of their intrinsic *BCR/ABL*-driven lymphoid-bias potential. CML development is accompanied by considerable changes in the pro-inflammatory tumor environment. Autocrine or paracrine mechanisms involving IL-3, G-CSF or GM-CSF have been reported to enhance the proliferation and viability of primitive CML cells both in mouse models and human samples (Jiang et al., 1999; Zhang and Ren, 1998). However, the real contribution of these pathways to CML development remains unclear as their inactivation in the mouse does not significantly affect disease outcome (Li et al., 2001). Here, we identify IL-6 as a key cytokine whose expression and secretion by myeloid cells is most affected by CML development, which confirms earlier findings in serum of CML patients (Anand et al., 1998) and very recent observations using the retroviral transduction/transplantation model of CML

(Schmidt et al., 2011). IL-6 exerts multiple, and some time divergent, functions on hematopoietic cells, including the provision of instructive cues for myeloid differentiation in normal contexts and in mouse models of inflammation or autoimmune diseases (Maeda et al., 2005; Maeda et al., 2009). Here, we show that the IL-6 receptor expression starts at the MPP stage of hematopoietic differentiation and is not affected by BCR/ABL activity. We demonstrate that IL-6 acts on both normal and leukemic MPPs to re-direct their differentiation potential towards the myeloid lineage at the expense of lymphoid differentiation. Furthermore, we show unambiguously by a genetic approach in the mouse that impairment of IL-6 signaling delays CML development, hence confirming the essential contribution of this pathway as a feedback loop supporting chronic phase CML. This paracrine mechanism appears exacerbated in CML myeloid blast crisis, most likely due to increased IL-6 production by blast cells as shown here by genome-wide genes expression analyses of CML patient samples. Disruption of the IL-6 paracrine loop, either through mutations in the IL-6 signaling pathway or loss of IL-6 production, and subsequent release of CML-MPP intrinsic B-lymphoid potential may also constitute the first step in the otherwise apparently random myeloid/lymphoid conversion observed during CML progression to lymphoid blast crisis. Instructive signals controlling the myeloid/lymphoid balance in CML is reminiscent to what has been described in MLL-rearranged AML, where growth factors and cytokines can instruct the lineage fate of multipotent LSCs (Barabe et al., 2007). Taken together, these findings demonstrate that blood cancers, like solid cancers, are profoundly affected by the pro-tumorigenic inflammatory environment in which leukemic stem and progenitor cells reside and function.

IL-6 signaling as a target for CML therapy

IL-6 has been previously implicated in the pathogenesis of hematological malignancies (*i.e.*, multiple myeloma, Hodgkin's lymphoma) and solid cancers (*i.e.*, breast, prostate and recently pancreatic cancers) (Hong et al., 2007). Here, we identify IL-6 as a major player in CML pathogenesis. We demonstrate that BCR/ABL activity dictates the level of IL-6 produced by both mouse and human myeloid CML cells. We show that BCR/ABL regulates *IL-6* mRNA levels through a complex and indirect mechanism involving, at least, BCL6 and the LIN28/28b-Let-7 pathway, which are two known transcriptional regulators of the *IL-6* gene (Iliopoulos et al., 2009; Yu et al., 2005). We find that pharmacological inhibition of BCR/ABL activity with TKIs restore *IL-6* expression and production to its normally low levels. We also show that disruption of the IL-6 paracrine loop through genetic ablation of the *Il-6* gene in mice significantly delays CML onset despite persistent BCR/ABL activity. These results suggest that therapies aimed at blocking IL-6 or targeting the IL-6 signal transduction pathway, although non-curative, could provided clinical benefits for CML patients that develop resistance to TKI treatment or undergo myeloid blast crisis progression. One important concern is that the aberrant B cell expansion driven by CML-MPPs and observed upon IL-6 inactivation may represent a pre-leukemic stage, which could evolve into an aggressive B-ALL upon acquisition of additional mutations (Mullighan et al., 2008). However, no lymphoid malignancies have spontaneously developed over time in aged *BA Il-6*$^{-/-}$ mice (n=17; data not shown), and we are currently performing additional genetic experiments in *BA Il-6*$^{-/-}$ mice to directly test this hypothesis and address the safety of IL-6 blocking therapies. Finally, it is tempting to speculate that such self-reinforcing paracrine loop involving IL-6, or other secreted pro-inflammatory factors, might be relevant in a broad spectrum of myeloid disorders. It opens the possibility of combinatorial strategies targeting not only the bulk tumor cells and the LSC compartment but also the pro-tumorigenic inflammatory environment, which controls the function of the leukemic hierarchy. Such a three-pronged approach might, in fact, be needed to develop curative treatment for CML and other types of blood malignancies.

EXPERIMENTAL PROCEDURES

Mice

Scl/Tal-1-tTA and *TRE-BCR/ABL* mice were backcrossed for at least 9 generations in the C57Bl/6 background and were interbred in presence of 20 mg/L doxycycline (Sigma-Aldrich) in their drinking water. *Il-6*$^{-/-}$ mice were purchased from the Jackson laboratory. Transplantations were performed as previously described (Santaguida et al., 2009). All animal experiments were performed in accordance with UCSF IACUC approved protocols.

Flow cytometry

Staining and enrichment procedures for stem and progenitor population sorting and analysis were performed as previously described (Santaguida et al., 2009). Cells were sorted or analyzed on a FACS ARIAII or LSRII (Becton Dickinson), respectively.

Cell culture

For myeloid differentiation assays, 500 MPPs or GMPs were plated in 10 mm dishes in methylcellulose (StemCell Technology, M3231) supplemented with SCF (25 ng/ml) and Flt3L (25 ng/ml) in the presence or absence of IL-6 (20 ng/ml) (Peprotech) and grown for 2 weeks. For B cell differentiation assays, cells were plated on OP9 stromal cells in OptiMEM medium (Invitrogen) supplemented with 5% FBS (StemCell Technology), SCF (10 ng/ml), Flt3L (10 ng/ml), and IL-7 (5 ng/ml). Following sequential withdrawal of Flt3L and SCF upon two-day intervals, cultures were maintained in IL-7 and analyzed at day 8 by flow cytometry. K562 and HL60 human cell lines were cultured for 15-20 hours in RPMI medium supplemented with 10% FBS in presence or absence of TKI (5 μM Imatinib or 100 nM Dasatinib).

Protein Array and ELISA

Antibody-based protein array (Proteome Profiler™, R&D Systems) and IL-6 ELISA assays (eBioscience) were performed on sera according to the manufacturer's instructions. The assay detection range was 5 to 1000 pg/ml.

Proliferation assays

Intracellular BrdU staining and 7AAD/Pyronin Y staining were performed as previously described (Santaguida et al., 2009).

Quantitative RT-PCR array

Quantitative RT-PCR arrays were performed on the Fluidigm 96.96 Dynamic Array IFC™ platform. Intron-spanning sets of primers for pre-amplification and quantitative PCR were validated on serial dilution of total mouse cDNA to ensure linear amplification, PCR specificity and performance. 100 cells were directly sorted in 5 μl of resuspension buffer from Cellsdirect™ One-Step qRT-PCR kits (Invitrogen). Samples were used for random hexamer-based reverse-transcription (SuperScript III™ kit, Invitrogen) and pre-amplified for 18 cycles with Platinium^{R} Taq DNA polymerase (Invitrogen) and primer mix (50 nM). Resulting cDNA products were analyzed on Fluidigm BioMark™ System using EvaGreen^{R} dye (Biotium). Each measurement was performed in triplicate and expression levels of *Gusb*, *Gapdh*, *Pgk1* and *Cltc* house keeping genes were used for normalization.

Microarray gene expression studies

Gene expression profiles of CML patient samples have been described previously (Radich et al., 2006, GEO accession number 4170). This published data set was analyzed for the

expression of IL-6 and BCL6 in BM and PB samples from 42 chronic, 17 accelerated and 32 blast crisis phase CML patients.

Statistics

All the data are expressed as mean ± standard error of the mean (error bar) except when indicated. *P* values were generated using unpaired Student's t-test and considered significant when ≤ 0.05. For survival curve, *p* values were generated using Mantel-Cox test. *N* indicates the numbers of independent experiments performed.

Supplementary Material

Refer to Web version on PubMed Central for supplementary material.

Acknowledgments

We thank Drs. N. Shah and S. Kogan (UCSF) and the members of the Passegué laboratory for critical reading of this manuscript; Dr. D. Tenen (Harvard University) for the generous gift of the *Scl/Tal-1-tTA* and *TRE-BCR/ABL* mice; K. Livak and A. Hamilton (Fluidigm Corporation) for providing expert assistance with qPCR analysis; T. Rambaldo and B. Hyun for management of our Flow Cytometry core facility; and the members of the UCSF Hematological Malignancy group for discussion and support. This work was supported by a Rita Allen Scholar award and NIH grant HL092471 to E.P. The authors have no financial interests to disclose.

REFERENCES

Anand M, Chodda SK, Parikh PM, Nadkarni JS. Abnormal levels of proinflammatory cytokines in serum and monocyte cultures from patients with chronic myeloid leukemia in different stages, and their role in prognosis. Hematol Oncol. 1998; 16:143–154. [PubMed: 10414234]

Barabe F, Kennedy JA, Hope KJ, Dick JE. Modeling the initiation and progression of human acute leukemia in mice. Science. 2007; 316:600–604. [PubMed: 17463288]

Barnes DJ, Melo JV. Primitive, quiescent and difficult to kill: the role of non-proliferating stem cells in chronic myeloid leukemia. Cell Cycle. 2006; 5:2862–2866. [PubMed: 17172863]

Benveniste P, Frelin C, Janmohamed S, Barbara M, Herrington R, Hyam D, Iscove NN. Intermediate-term hematopoietic stem cells with extended but time-limited reconstitution potential. Cell Stem Cell. 2010; 6:48–58. [PubMed: 20074534]

Buesche G, Ganser A, Schlegelberger B, von Neuhoff N, Gadzicki D, Hecker H, Bock O, Frye B, Kreipe H. Marrow fibrosis and its relevance during imatinib treatment of chronic myeloid leukemia. Leukemia. 2007; 21:2420–2427. [PubMed: 17805334]

Corbin AS, Agarwal A, Loriaux M, Cortes J, Deininger MW, Druker BJ. Human chronic myeloid leukemia stem cells are insensitive to imatinib despite inhibition of BCR-ABL activity. J Clin Invest. 2011; 121:396–409. [PubMed: 21157039]

Duy C, Hurtz C, Shojaee S, Cerchietti L, Geng H, Swaminathan S, Klemm L, Kweon SM, Nahar R, Braig M, et al. BCL6 enables Ph+ acute lymphoblastic leukaemia cells to survive BCR-ABL1 kinase inhibition. Nature. 2011; 473:384–388. [PubMed: 21593872]

Holyoake T, Jiang X, Eaves C, Eaves A. Isolation of a highly quiescent subpopulation of primitive leukemic cells in chronic myeloid leukemia. Blood. 1999; 94:2056–2064. [PubMed: 10477735]

Hong DS, Angelo LS, Kurzrock R. Interleukin-6 and its receptor in cancer: implications for Translational Therapeutics. Cancer. 2007; 110:1911–1928. [PubMed: 17849470]

Hu Y, Swerdlow S, Duffy TM, Weinmann R, Lee FY, Li S. Targeting multiple kinase pathways in leukemic progenitors and stem cells is essential for improved treatment of Ph+ leukemia in mice. Proc Natl Acad Sci U S A. 2006; 103:16870–16875. [PubMed: 17077147]

Huntly BJ, Shigematsu H, Deguchi K, Lee BH, Mizuno S, Duclos N, Rowan R, Amaral S, Curley D, Williams IR, et al. MOZ-TIF2, but not BCR-ABL, confers properties of leukemic stem cells to committed murine hematopoietic progenitors. Cancer Cell. 2004; 6:587–596. [PubMed: 15607963]

Iliopoulos D, Hirsch HA, Struhl K. An epigenetic switch involving NF-kappaB, Lin28, Let-7 MicroRNA, and IL6 links inflammation to cell transformation. Cell. 2009; 139:693–706. [PubMed: 19878981]

Jiang X, Lopez A, Holyoake T, Eaves A, Eaves C. Autocrine production and action of IL-3 and granulocyte colony-stimulating factor in chronic myeloid leukemia. Proc Natl Acad Sci U S A. 1999; 96:12804–12809. [PubMed: 10536003]

Klinakis A, Lobry C, Abdel-Wahab O, Oh P, Haeno H, Buonamici S, van De Walle I, Cathelin S, Trimarchi T, Araldi E, et al. A novel tumour-suppressor function for the Notch pathway in myeloid leukaemia. Nature. 2011; 473:230–233. [PubMed: 21562564]

Kopf M, Baumann H, Freer G, Freudenberg M, Lamers M, Kishimoto T, Zinkernagel R, Bluethmann H, Kohler G. Impaired immune and acute-phase responses in interleukin-6-deficient mice. Nature. 1994; 368:339–342. [PubMed: 8127368]

Koschmieder S, Gottgens B, Zhang P, Iwasaki-Arai J, Akashi K, Kutok JL, Dayaram T, Geary K, Green AR, Tenen DG, Huettner CS. Inducible chronic phase of myeloid leukemia with expansion of hematopoietic stem cells in a transgenic model of BCRABL leukemogenesis. Blood. 2005; 105:324–334. [PubMed: 15331442]

Li S, Gillessen S, Tomasson MH, Dranoff G, Gilliland DG, Van Etten RA. Interleukin 3 and granulocyte-macrophage colony-stimulating factor are not required for induction of chronic myeloid leukemia-like myeloproliferative disease in mice by BCR/ABL. Blood. 2001; 97:1442–1450. [PubMed: 11222392]

Maeda K, Baba Y, Nagai Y, Miyazaki K, Malykhin A, Nakamura K, Kincade PW, Sakaguchi N, Coggeshall KM. IL-6 blocks a discrete early step in lymphopoiesis. Blood. 2005; 106:879–885. [PubMed: 15831701]

Maeda K, Malykhin A, Teague-Weber BN, Sun XH, Farris AD, Coggeshall KM. Interleukin-6 aborts lymphopoiesis and elevates production of myeloid cells in systemic lupus erythematosus-prone B6.Sle1.Yaa animals. Blood. 2009; 113:4534–4540. [PubMed: 19224760]

Mullighan CG, Miller CB, Radtke I, Phillips LA, Dalton J, Ma J, White D, Hughes TP, Le Beau MM, Pui CH, et al. BCR-ABL1 lymphoblastic leukaemia is characterized by the deletion of Ikaros. Nature. 2008; 453:110–114. [PubMed: 18408710]

Passegue E, Weissman IL. Leukemic stem cells: where do they come from? Stem Cell Rev. 2005; 1:181–188. [PubMed: 17142854]

Perrotti D, Jamieson C, Goldman J, Skorski T. Chronic myeloid leukemia: mechanisms of blastic transformation. J Clin Invest. 2010; 120:2254–2264. [PubMed: 20592475]

Pietras EM, Warr M, Passegué E. Cell cycle regulation in hematopoietic stem cells. J Cell Biol. 2011 In press.

Porosnicu M, Nimmanapalli R, Nguyen D, Worthington E, Perkins C, Bhalla KN. Co-treatment with As2O3 enhances selective cytotoxic effects of STI-571 against Brc-Abl-positive acute leukemia cells. Leukemia. 2001; 15:772–778. [PubMed: 11368438]

Radich JP, Dai H, Mao M, Oehler V, Schelter J, Druker B, Sawyers C, Shah N, Stock W, Willman CL, et al. Gene expression changes associated with progression and response in chronic myeloid leukemia. Proc Natl Acad Sci U S A. 2006; 103:2794–2799. [PubMed: 16477019]

Santaguida M, Schepers K, King B, Sabnis AJ, Forsberg EC, Attema JL, Braun BS, Passegue E. JunB protects against myeloid malignancies by limiting hematopoietic stem cell proliferation and differentiation without affecting self-renewal. Cancer Cell. 2009; 15:341–352. [PubMed: 19345332]

Savona M, Talpaz M. Getting to the stem of chronic myeloid leukaemia. Nat Rev Cancer. 2008; 8:341–350. [PubMed: 18385684]

Schemionek M, Elling C, Steidl U, Baumer N, Hamilton A, Spieker T, Gothert JR, Stehling M, Wagers A, Huettner CS, et al. BCR-ABL enhances differentiation of long-term repopulating hematopoietic stem cells. Blood. 2010; 115:3185–3195. [PubMed: 20053753]

Schmidt T, Kharabi Masouleh B, Loges S, Cauwenberghs S, Fraisl P, Maes C, Jonckx B, De Keersmaecker K, Kleppe M, Tjwa M, et al. Loss or Inhibition of Stromal-Derived PlGF Prolongs Survival of Mice with Imatinib-Resistant Bcr-Abl1(+) Leukemia. Cancer Cell. 2011; 19:740–753. [PubMed: 21665148]

Viswanathan SR, Powers JT, Einhorn W, Hoshida Y, Ng TL, Toffanin S, O'Sullivan M, Lu J, Phillips LA, Lockhart VL, et al. Lin28 promotes transformation and is associated with advanced human malignancies. Nat Genet. 2009; 41:843–848. [PubMed: 19483683]

Warr MR, Pietras EM, Passegue E. Mechanisms controlling hematopoietic stem cell functions during normal hematopoiesis and hematological malignancies. Wiley Interdiscip Rev Syst Biol Med. 2011

Yu RY, Wang X, Pixley FJ, Yu JJ, Dent AL, Broxmeyer HE, Stanley ER, Ye BH. BCL-6 negatively regulates macrophage proliferation by suppressing autocrine IL-6 production. Blood. 2005; 105:1777–1784. [PubMed: 15507530]

Zhang B, Strauss AC, Chu S, Li M, Ho Y, Shiang KD, Snyder DS, Huettner CS, Shultz L, Holyoake T, Bhatia R. Effective targeting of quiescent chronic myelogenous leukemia stem cells by histone deacetylase inhibitors in combination with imatinib mesylate. Cancer Cell. 2010; 17:427–442. [PubMed: 20478526]

Zhang X, Ren R. Bcr-Abl efficiently induces a myeloproliferative disease and production of excess interleukin-3 and granulocyte-macrophage colony-stimulating factor in mice: a novel model for chronic myelogenous leukemia. Blood. 1998; 92:3829–3840. [PubMed: 9808576]

SIGNIFICANCE

Here, we show that the clinically relevant CML-LSCs are solely contained in the LT-HSC compartment, and identify aberrant features of these cells that could be amendable to targeted therapy. We find that CML-LSCs are hyperproliferative and outcompete normal LT-HSCs due to major alterations in their cell cycle control and deregulation of the Notch pathway. Moreover, we identify two leukemic progenitors, which are devoid of self-renewal activity but are critical for CML pathogenesis. We demonstrate that BCR/ABL controls expression of the pro-inflammatory cytokine IL-6 and establishes a paracrine loop acting on leukemic MPPs to promote myeloid development at the expense of lymphoid differentiation. This finding adds IL-6 blocking therapy as a potential strategy to control CML development.

HIGHLIGHTS

- Leukemic multipotent progenitors contribute to CML pathogenesis
- The pro-tumorigenic inflammatory environment modulates CML development
- BCR/ABL controls *IL-6* expression levels in myeloid CML cells
- IL-6 dictates lineage specification in CML multipotent progenitors

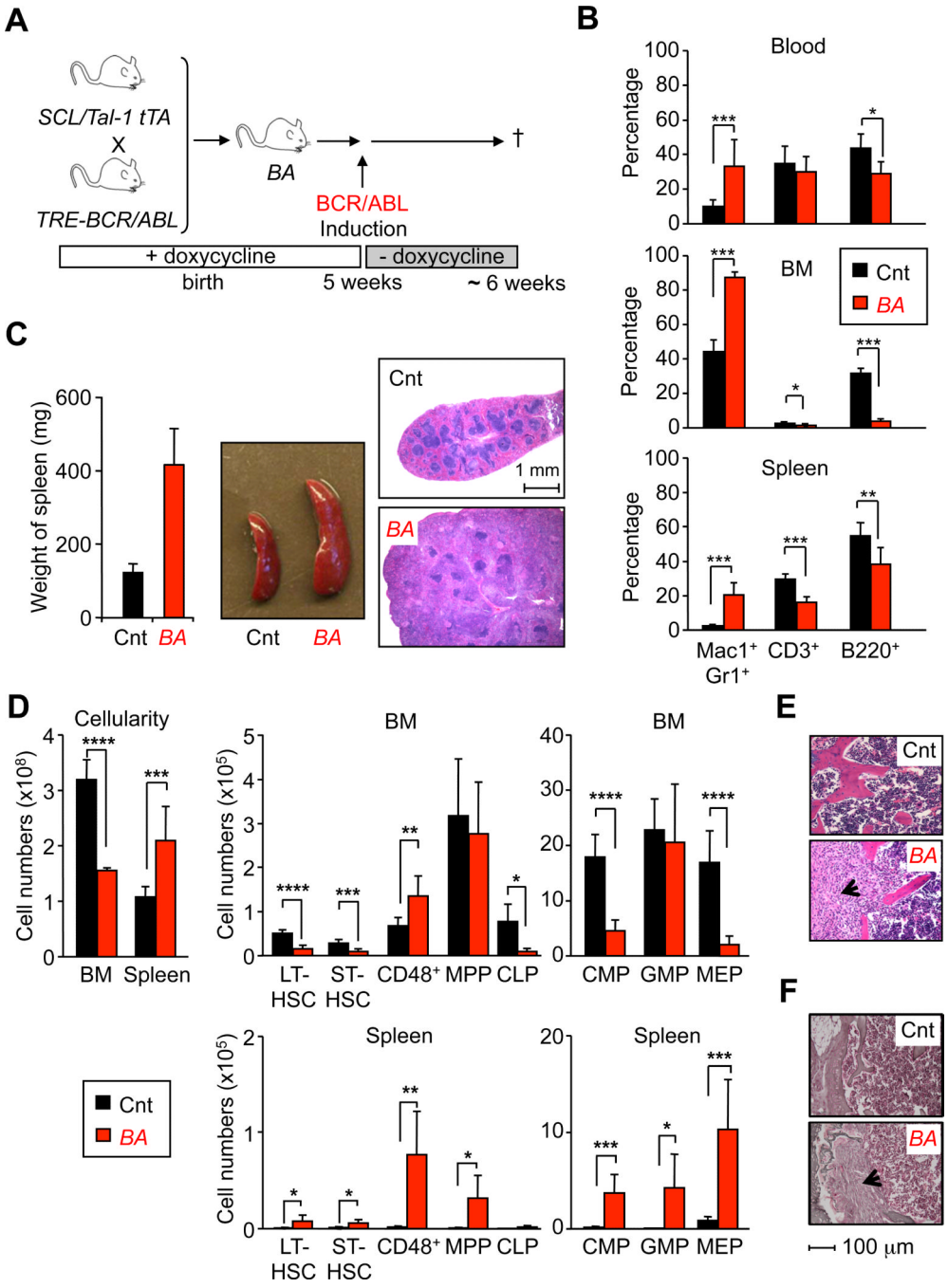

Figure 1. CML hematopoiesis in inducible BCR/ABL transgenic mice

(**A**) Experimental scheme. Double transgenic mice (*BA*) were maintained in presence of doxycycline (20mg/L) in drinking water until 5 weeks of age before inducting *BCR/ABL* by doxycycline withdrawal. Wild type and single transgenic littermates treated with the same regimen were used as controls (Cnt) and all the mice were analyzed 6 weeks after doxycycline withdrawal.

(B) Hematopoietic features in CML mice. Graphs show the percentages of mature cells detected in PB, BM and spleen of Cnt and *BA* mice. Results are expressed as mean ± SD ($n \geq 8$; $*p \leq 10^{-2}$, $**p \leq 10^{-3}$, $***p \leq 10^{-4}$).

(C) Weight, morphology and hematoxylin and eosin (H&E) staining of spleen from Cnt and *BA* mice.

(**D**) Total cellularity and cell number for each progenitor compartment in BM and spleen of Cnt and *BA* mice. Results are expressed as mean ± SD (n≥6; *$p \leq 10^{-2}$, **$p \leq 10^{-3}$, ***$p \leq 10^{-4}$, **** $p \leq 10^{-5}$).

(**E**) H&E and (**F**) Gordon and Sweet's reticulin staining of BM (sternum) section from Cnt and *BA* mice. The arrowhead indicates myelofibrotic tissue

See also Figure S1.

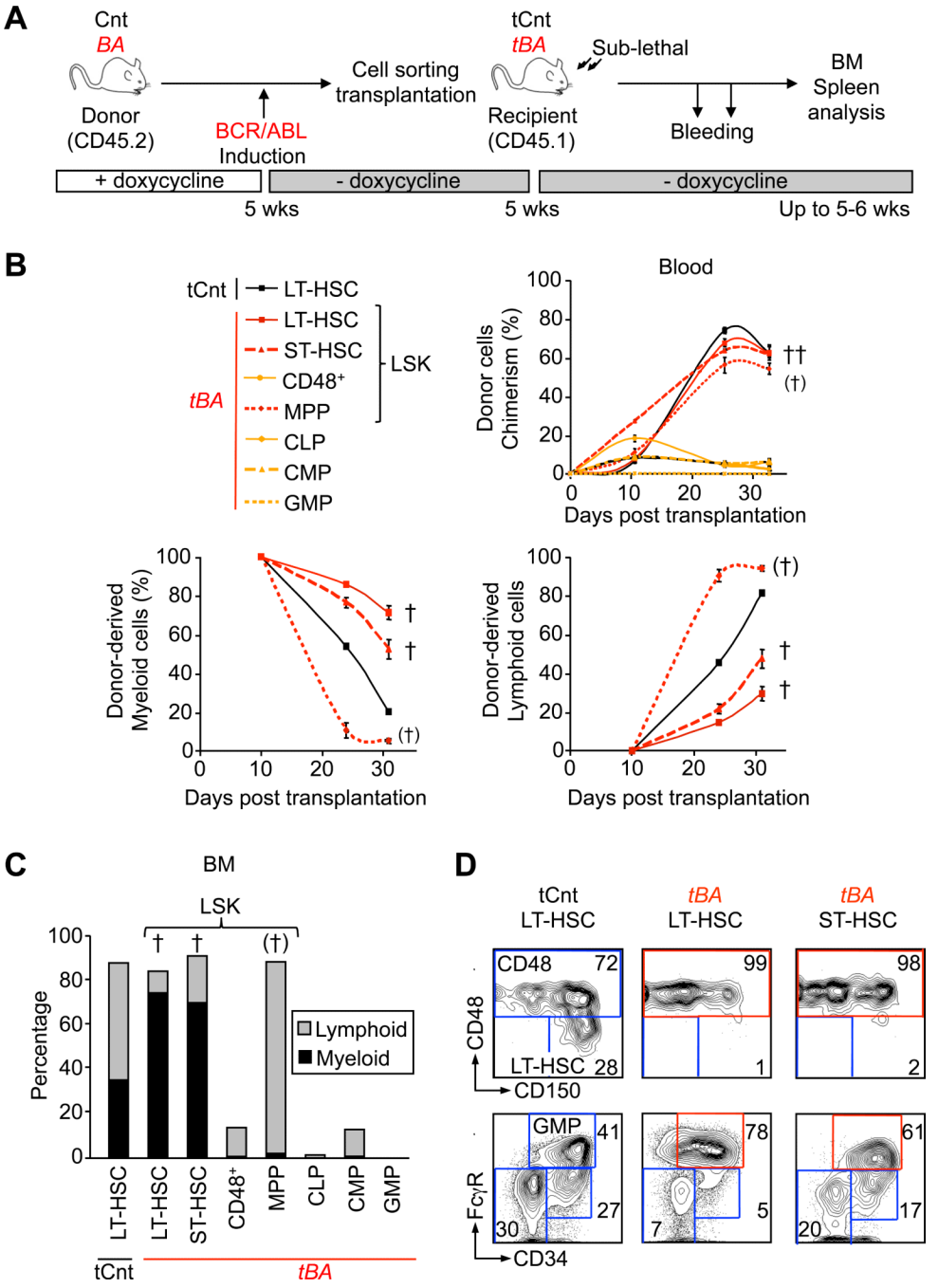

Figure 2. Refining the identity of CML leukemic stem cells

(**A**) Experimental scheme. Cells were isolated by flow cytometry from Cnt or *BA* mice (CD45.2) 5 weeks after doxycycline withdrawal. 4,000 (LT-HSC, ST-HSC, CD48, MPP and CLP) or 40,000 (CMP and GMP) cells were transplanted into sub-lethally irradiated CD45.1 recipients (denoted tCnt and *tBA*). Transplanted mice were bled at several time points, and BM analyses were performed at 35 days post-transplantation.

(**B**) Kinetics of hematopoietic reconstitution in PB. The upper graph indicates the overall percentage of CD45.2 chimerism. The lower left and right graphs show the percentage of donor-derived myeloid ($Mac1^+$) and lymphoid ($B220^+/CD3^+$) cells, respectively. Results are

expressed as mean ± SEM (n=2-6). † indicates cohorts found moribund at the time of analysis. (†) indicates cohort with partial mortality (2 out of 7).
(**C**) Hematopoietic reconstitution in BM. Histograms show the average percentage (n=2-5) of donor-derived myeloid ($Mac1^+$, black) and lymphoid ($B220^+/CD3^+$, grey) cells.
(**D**) Reorganization of the immature BM compartments in transplanted mice. Representative FACS plots showing the change in frequency in mice transplanted with 4,000 Cnt or BA^+ LT-HSCs and ST-HSCs.
See also Figure S2.

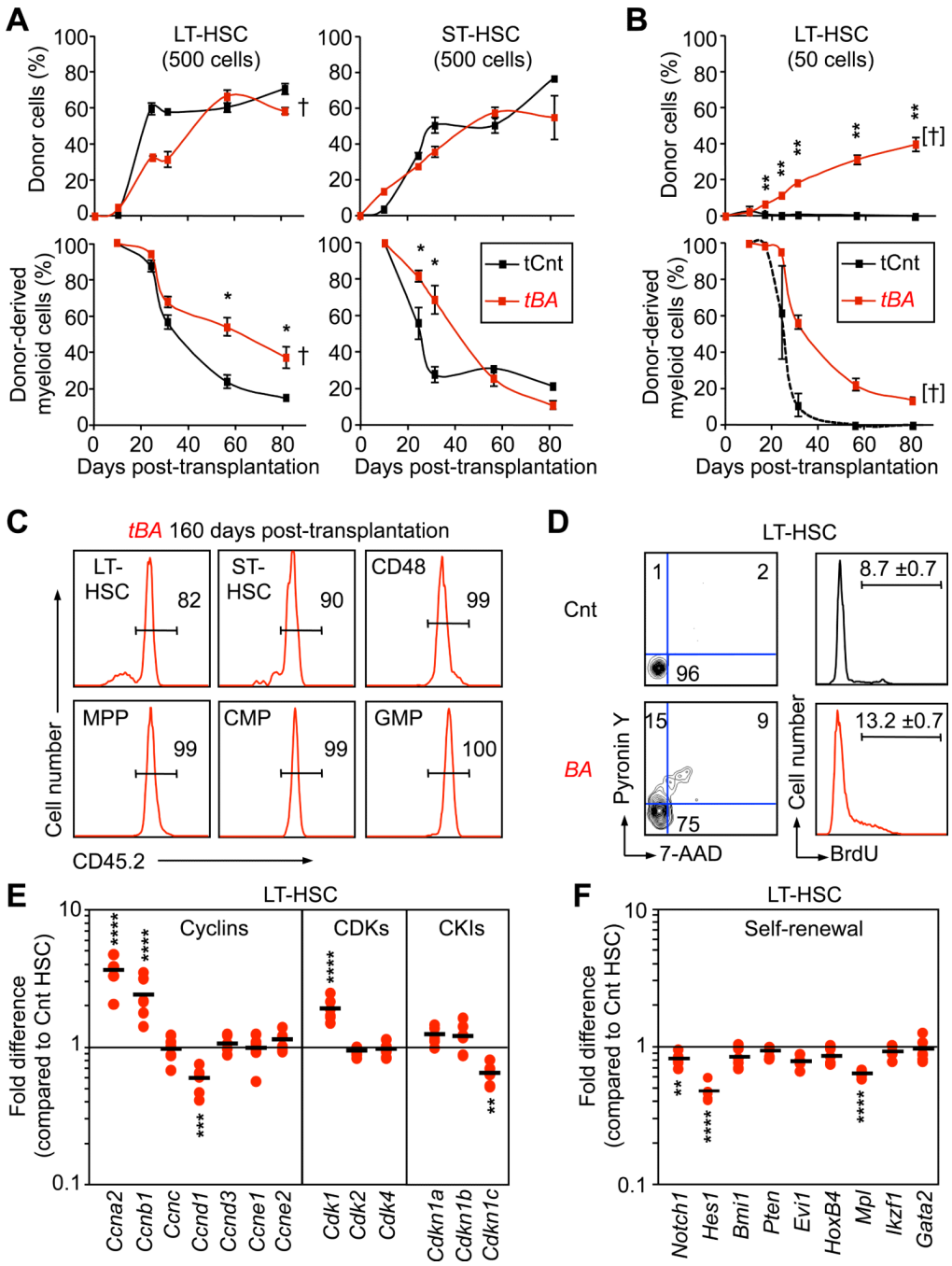

Figure 3. Functional and molecular characterization of CML leukemic stem cells

(**A**) Leukemic potential of CML LT-HSCs and ST-HSCs. Cells were isolated from Cnt and *BA* mice (CD45.2) 5 weeks after doxycycline withdrawal and transplanted (500 cells/mouse) into sub-lethally irradiated recipients (CD45.1). Transplanted mice were bled at several time points and analyzed for overall percentage of CD45.2 chimerism (upper graphs) and percent of donor-derived Mac1^{+} myeloid cells (lower graphs). Results are expressed as mean ± SEM (n=2-3; *p≤5×10^{-2}). † indicates cohorts found moribund.

(**B**) Limiting dilution transplantation. 50 Cnt or *BA*$^{+}$ LT-HSCs (CD45.2) were transplanted into sub-lethally irradiated recipients (CD45.1) together with 3×10^{5} Sca-1-depleted BM cells (CD45.1). Graphs show kinetics of hematopoietic reconstitution in PB and results are

expressed as mean ± SEM (n=7; **p≤10^{-3}). [†] indicates cohort found moribund at later time points. **(C)** Clonal expansion analyses. The panels show representative examples of the percentage of CD45.2 chimerism in BM compartments 160 days after transplantation of 50 *BA*$^{+}$ LT-HSCs.

(**D**) Cell-cycle analyses. LT-HSCs were isolated from Cnt and *BA* mice 5 weeks after doxycycline withdrawal. The left panels show DNA/RNA contents analyzed by 7-AAD and Pyronin Y (PY) staining, and the right panels shows BrdU incorporation in cells cultured for 1 hour with 60 μM BrdU. Results are expressed as mean ± SEM (n=2)

(**E**) and (**F**) Quantitative gene expression analyses. Pools of 100 Cnt and *BA*$^{+}$ LT-HSCs were analyzed on a Fluidigm Dynamic Array IFC for a custom made set of cell cycle and self-renewal genes, respectively. Results are expressed as fold change relative to Cnt LT-HSCs (n=7; **p≤10^{-3}, ***p≤10^{-4}, **** p≤10^{-5}).

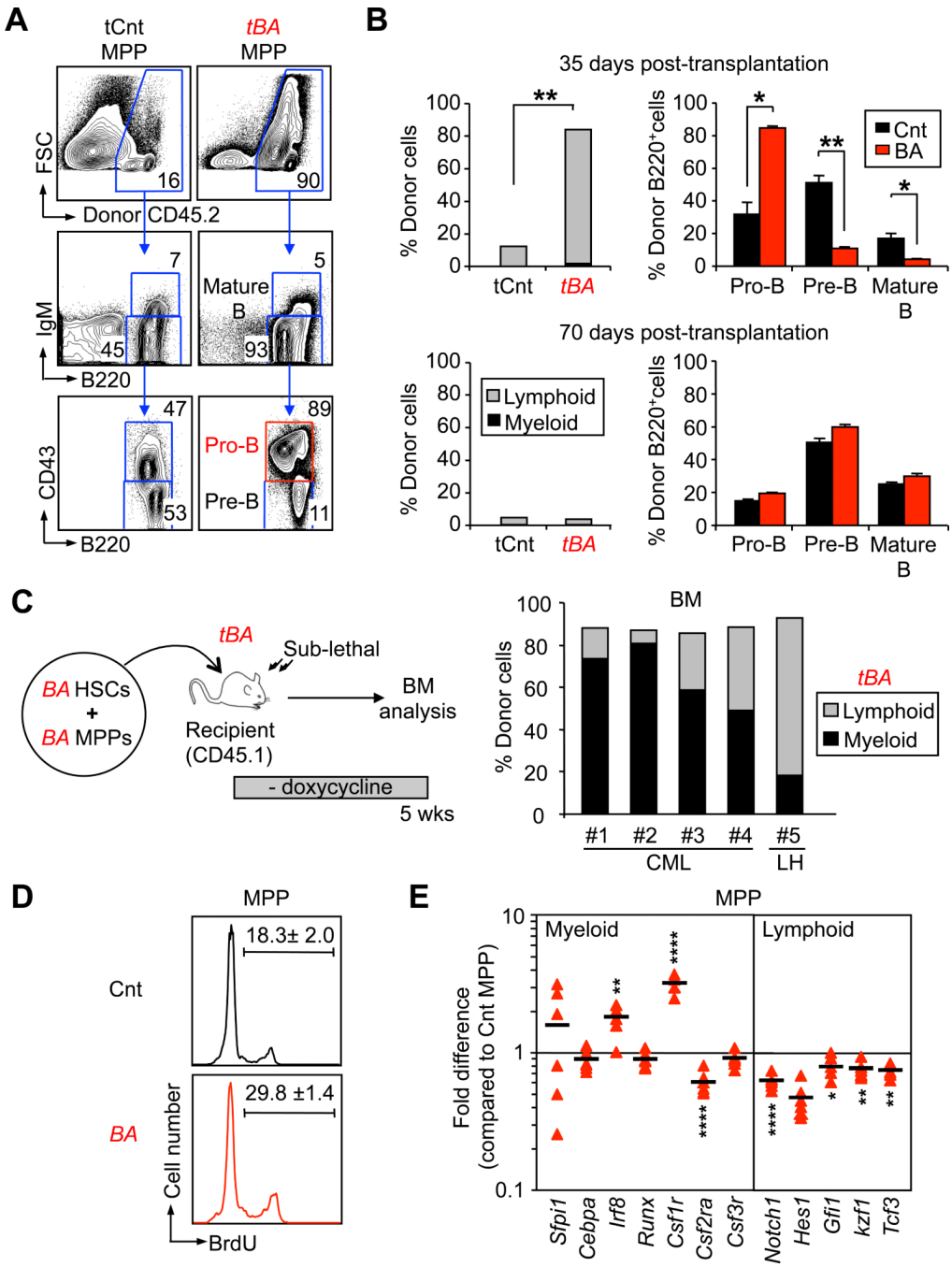

Figure 4. Context-dependent behavior of leukemic MPPs

(**A**) Reconstitution potential of CML MPPs. 4,000 Cnt or *BA*$^+$ MPPs (CD45.2) were transplanted into sub-lethally irradiated recipient mice (CD45.1). Recipients (n=5) were sacrificed and BM reconstitution was analyzed by flow cytometry 35 days post-transplantation. Representative FACS plots showing an example of B cell progenitor reconstitution.

(**B**) Kinetics of B cell production in recipient BM at 35 (top panels) and 70 (bottom panels) days post-transplantation. The left graphs indicate the average percentage of donor-derived myeloid (Mac1$^+$, black) and lymphoid (B220$^+$/CD3$^+$, grey) cells. The right graphs show the percentage of CD43$^+$/IgM$^-$ pro-B, CD43$^-$/IgM$^-$ pre-B and IgM$^+$ mature B cells in the

donor-derived $B220^+$ cells. Results are expressed as mean ± SEM (n=2-5; *$p \leq 5\times10^{-2}$, **$p \leq 5\times10^{-3}$).

(**C**) *In vivo* competition between leukemic compartments. 4,000 BA^+ HSCs (either LT-HSCs or ST-HSCs) together with 4,000 BA^+ MPPs (both CD45.2) were co-transplanted into sub-lethally irradiated recipient mice (CD45.1). The right graph shows the percentage of donor-derived myeloid and lymphoid cells in the BM of recipient mice 35 days post-transplantation. Of note, 4/5 mice developed a myeloid disease (CML) and 1 mouse a lymphoid hyperplasia (LH).

(**D**) Cell-cycle distribution. BrdU incorporation in MPPs isolated from Cnt and *BA* mice 5 weeks after doxycycline withdrawal and cultured for 1 hour with 60 μM BrdU. Results are expressed as mean ± SEM (n=2)

(**E**) Quantitative gene expression analyses. Pools of 100 Cnt and BA^+ MPPs were analyzed on a Fluidigm Dynamic Array IFC for a custom made set of genes regulating myeloid *vs*. lymphoid lineage specification. Results are expressed as fold change relative to Cnt MPPs (n=7; *$p \leq 10^{-2}$, **$p \leq 10^{-3}$, **** $p \leq 10^{-5}$).

See also Figure S3.

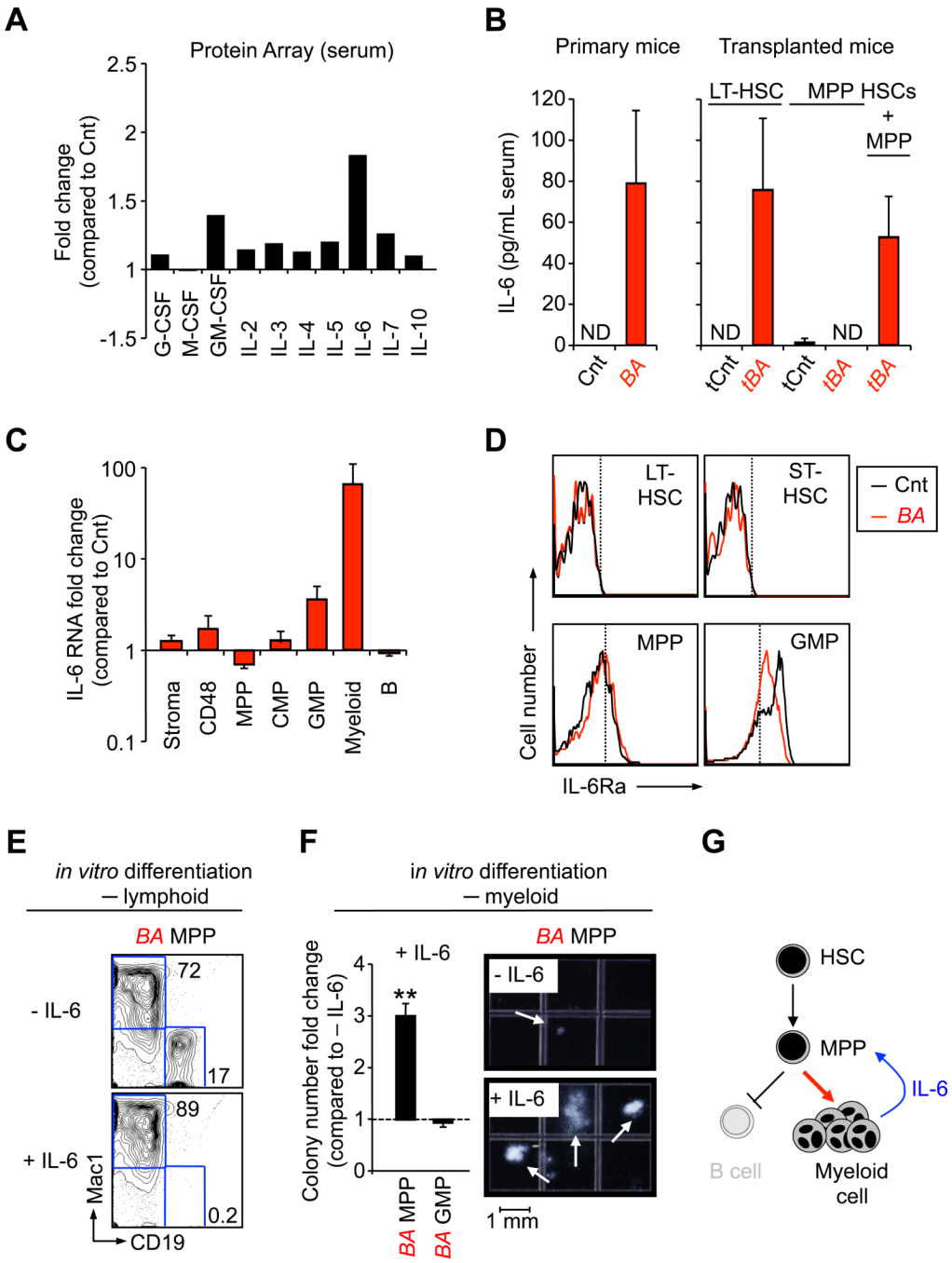

Figure 5. IL-6 paracrine loop

(**A**) Pro-tumorigenic inflammatory environment during CML development. Changes in the indicated growth factors and interleukin levels were determined using an antibody-based protein array on pools of sera from 16 Cnt and 7 *BA* mice 6 weeks after doxycycline withdrawal. Results are expressed as fold change relative to levels measured in Cnt mice (set to 1).

(**B**) Modulation of serum IL-6 levels. ELISA measurement of IL-6 concentration in serum of individual Cnt and *BA* primary mice (left graphs), and mice transplanted with the indicated populations (right graphs). Results are expressed as mean ± SEM (n=2-6). ND stands for "not detectable".

(C) qRT-PCR analysis of non-hematopoietic BM cells (stroma), CD48, MPP, CMP, GMP, mature myeloid and B cells for *Il-6* mRNA levels. Results are expressed as mean ± SEM (n=3).
(D) Representative FACS histograms showing expression of the α-chain of IL-6 receptor on the indicated Cnt (black) and BA^+ (red) populations. Dashed lines show isotype control negative boundaries. Data are representative of two independent experiments.
(**E**) Effect of IL-6 on lymphoid differentiation from BA^+ MPPs. The FACS plots show a representative phenotypic analysis of CD19 (lymphoid) and Mac-1 (myeloid) markers after 8 days of *in vitro* culture (n=2).
(**F**) Differential effect of IL-6 on myeloid differentiation from BA^+ MPPs and GMPs. The graph on the left show the fold changes in colony numbers when comparing conditions with or without IL-6 (set to 1). Results are expressed as mean ± SEM (n=2-3; $^{**}p \leq 5\times10^{-4}$). The photographs on the right show representative myeloid colonies generated in both conditions from BA^+ MPPs after 10 days of *in vitro* culture.
(**G**) Model describing the IL-6 paracrine loop in CML development identified in this study.

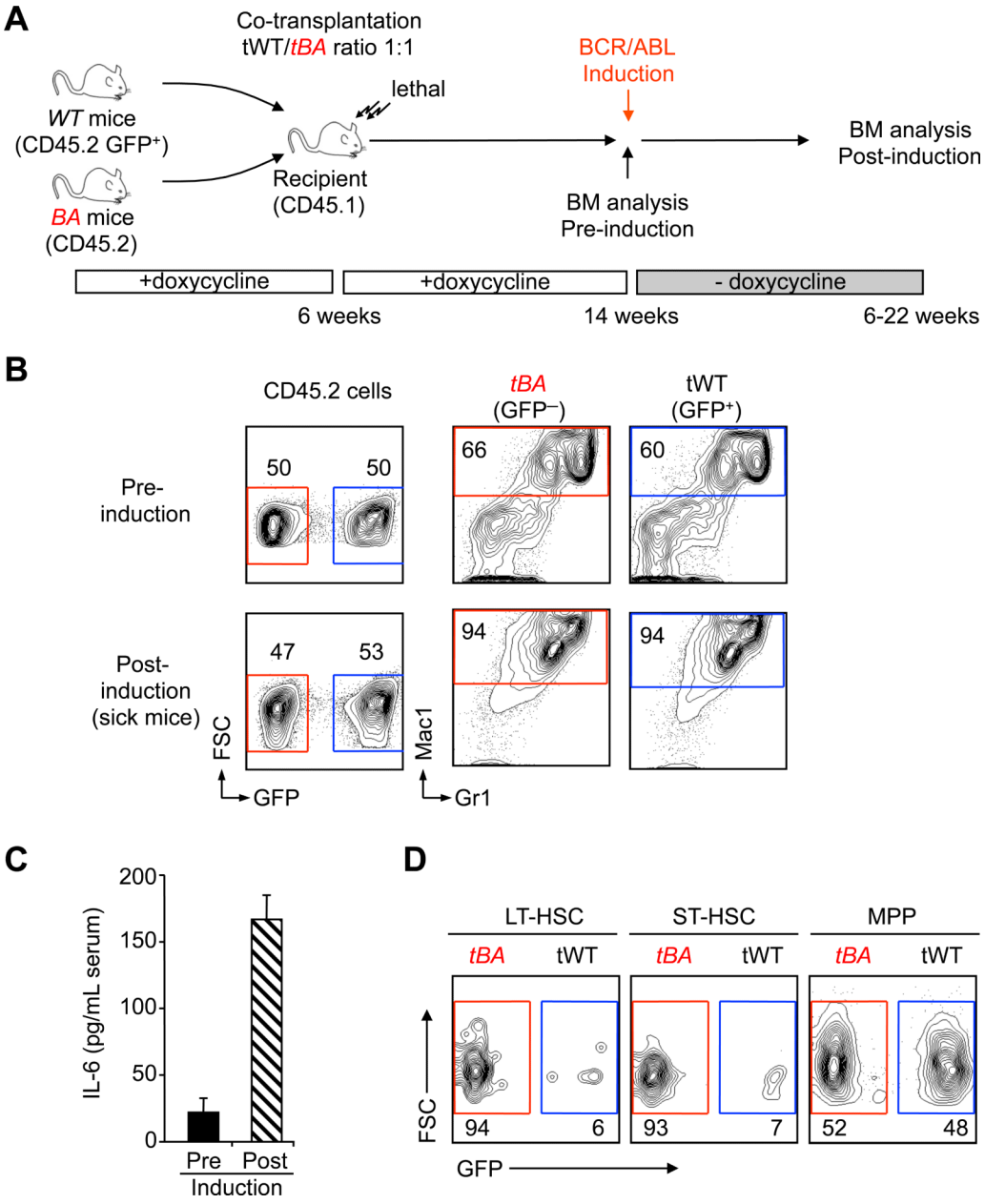

Figure 6. Contribution of IL-6 to lineage determination *in vivo*

(**A**) Experimental scheme. 5×10^6 wild type (tWT: CD45.2 GFP$^+$) and 5×10^6 non-induced *BA*$^+$(CD45.2 GFP$^-$) BM cells were co-transplanted into lethally irradiated recipients (CD45.1). Transplanted mice were maintained on doxycycline for 2 months to achieve stable reconstitution before inducing *BA* expression by doxycycline withdrawal. Mice were analyzed either pre or post *BA*-induction, when mice displayed signs of CML disease.

(**B**) Representative FACS plots showing contribution of tWT and *tBA* cells to the myeloid (Mac1$^+$/Gr1$^+$) BM output pre (top) and post (bottom) induction (n≥2).

(**C**) Concentration of IL-6 in the serum of transplanted mice pre and post induction. Results are expressed as mean ± SEM (n=2-4).

(**D**) Representative FACS plots showing contribution of tWT and *tBA* cells to the indicated BM compartments post induction (n=2).

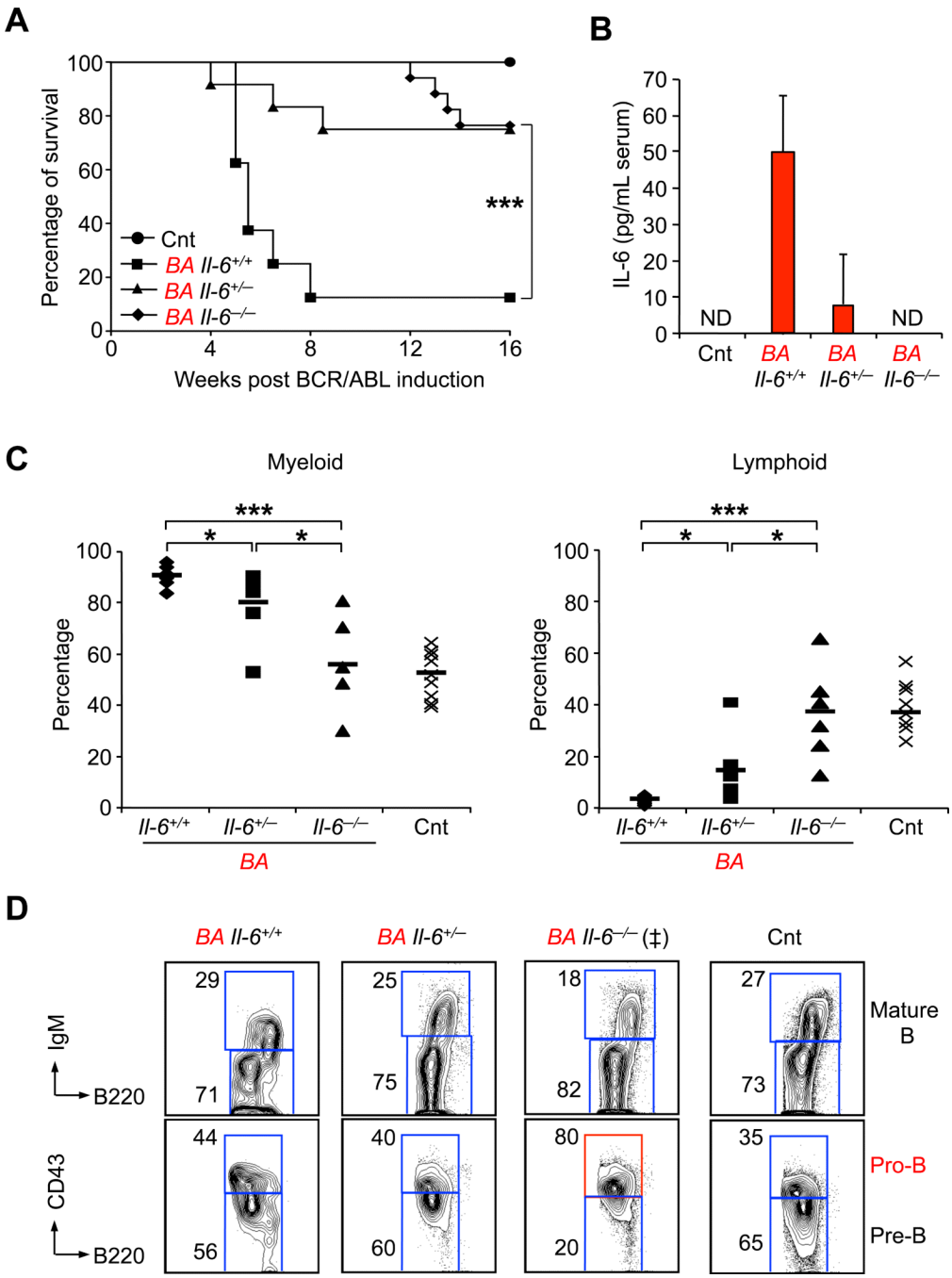

Figure 7. Role of IL-6 in CML development

(**A**) Survival curve of Cnt (n=11) and *Il-6*$^{+/+}$ (n=11), *Il-6*$^{+/-}$ (n=12) and *Il-6*$^{-/-}$ (n=17) *BA* mice after doxycyline withdrawal (*p≤ 5×10^{-2}).

(**B**) ELISA measurement of serum IL-6 levels in Cnt and *Il-6*$^{+/+}$, *Il-6*$^{+/-}$ and *Il-6*$^{-/-}$ *BA* mice. Results are expressed as mean ± SEM (n=7). ND stands for “not detectable”.

(**C**) Percentage of Mac1^{+} myeloid (left) and B220^{+} B-lymphoid (right) cells in BM of individual control and *Il-6*$^{+/+}$, *Il-6*$^{+/-}$ and *Il-6*$^{-/-}$ *BA* mice (n=5-10; *p≤ 5×10^{-2}, ***p≤5×10^{-4}).

(**D**) Representative FACS plots showing the phenotype of B cell progenitors generated in Cnt and *Il-6*$^{+/+}$, *Il-6*$^{+/-}$ and *Il-6*$^{-/-}$ *BA* mice. (‡) indicates that FACS plots is representative of 3 out of 5 analyzed mice with this genotype.

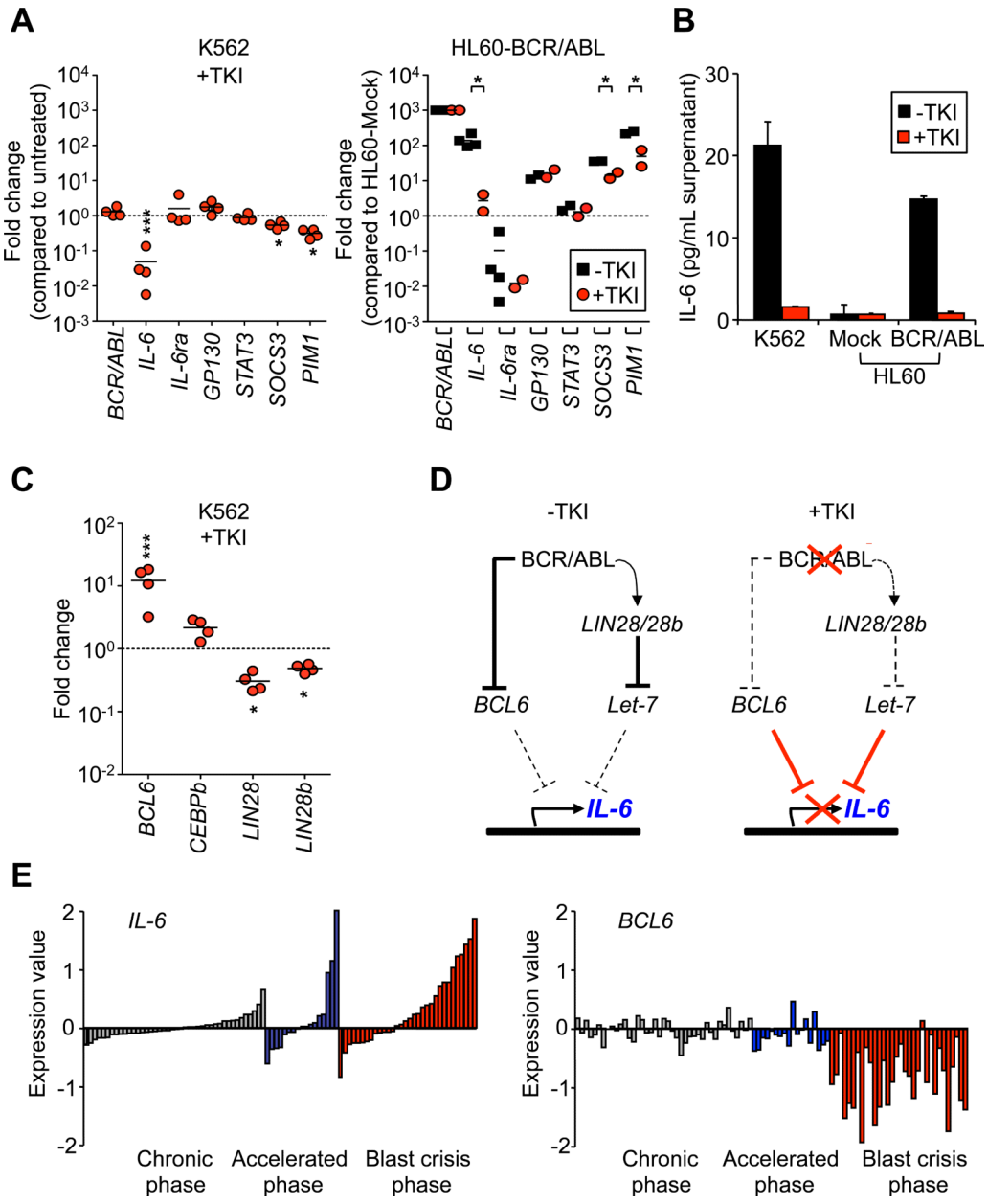

Figure 8. BCR/ABL controls Il-6 expression

(**A**) *BCR/ABL*-dependent *IL-6* expression in human cell lines. qRT-PCR analysis of IL-6 pathway components in K562 (left) and *BCR/ABL*-expressing HL60 (right) cells with or without TKI treatment. Results (mean; n=2-4) are expressed as fold change relative to untreated K562 (left) or Mock-transfected HL60 (right) cells (mean; n=2-4; *p<0.05).

(**B**) ELISA measurement of IL-6 concentration in the supernatant of the cell lines used in (A). Results are expressed as mean ± SEM (n=2)

(**C**) qRT-PCR analysis of BCR/ABL signaling pathway components in K562 cells with or without TKI treatment. Results (mean; n=4) are expressed as fold change relative to untreated K562 (left) cells.

(**D**) Proposed model for BCR/ABL regulation of *IL-6* expression. In CML cells, BCR/ABL activates Lin28 expression that blocks Let-7 microRNA maturation (Iliopoulos et al., 2009) and/or blocks *BCL6* expression (Duy et al., 2011) hence allowing transcription of the *IL-6*

gene. Inhibition of BCR/ABL activity by TKI treatment reduces Lin28 expression and/or releases BCL6 hence allowing them to blocks *IL-6* expression (Yu et al., 2005).
(**E**) Expression of IL-6 ($p<0.05$) and BCL6 ($p<0.0001$) in BM or PB from chronic (grey), accelerated (blue), and blast crisis (red) phase CML patients relative to the expression in a pool of 200 chronic phase patients. Expression is in logarithmic scale. Data was analyzed using Qlucore Omics Explorer (Qlucore, AB, Lund, Sweden). The software performs a multi group comparison using the ANOVA F-test.